SWITCHED RELUCTANCE VERSUS PERMANENT MAGNET

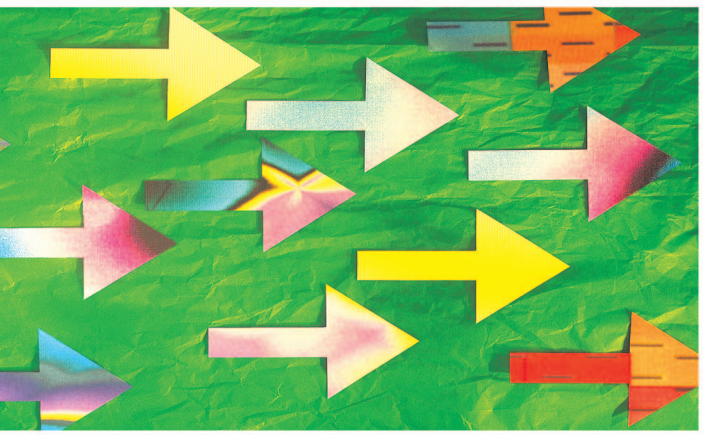

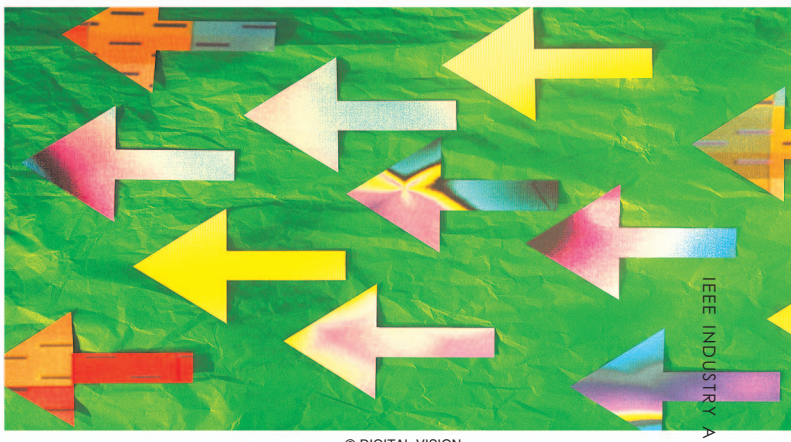

A comparison in the context of electric brakes

ELECTROMECHANICAL BRAKE (EMB) SYSTEMS OFFER THE potential for enhanced vehicle control while simplifying the car assembly as well as recycling processes [1], [2]. Vehicle control enhancements stem from the relative controllability ease of electrical systems but are predicated on a highly dynamic behavior from the motor drive. This article offers a comparison of two motor technologies, switched reluctance (SR) and permanent magnet (PM) brushless, for this particular application.

Digital Object Identifier 10.1109/MIAS.2009.932595

BY AVOKI M. OMEKANDA, BRUNO LEQUESNE, HARALD KLODE, SURESH GOPALAKRISHNAN, & IQBAL HUSAIN

1077-2618/09/$25.00©2009 IEEE

SR and PM Brushless Drive Systems

SR and PM-brushless drive systems have been compared in various papers in the past [3]–[5]. Each situation, however, has its own particularities, and in the present work the emphasis is on a highly dynamic, four-quadrant operation. Other important aspects of brakes that emerge during a comparison of these two technologies are either known or presented separately. The advantages of the SR motor in terms of temperature [6] and fault tolerance [3] need not be repeated. Other publications related to this project have described efforts to reduce the SR-drive cost and to bring it to the level of PM brushless drives or better. These cost-reduction studies focused on position-sensor elimination [7], [8], inverter switch-number reduction [9]–[11], and air-gap control and motor manufacturing [12]. In another respect, a study is presently underway concerning audible noise.

The EMB system investigated in this article consists of a rotary motor coupled to a planetary gear and ball-screw assembly that converts the motor torque and rotation into linear force and travel suitable for operation in a caliper brake (Figures 1 and 2) [13], [14]. The comparison was based on designing the two motors to meet identical torque-speed specifications (0.8 N·m up to a base speed of 1,500 r/min). Concerning packaging, there was a similar constraint on the outer diameter so that both motors would fit within the same hardware, but with some freedom concerning length.

The article first describes the motor designs and their static characteristics, before examining in some depth their dynamic behavior, in particular special control adaptations to enable the SR motor to reverse rapidly when needed.

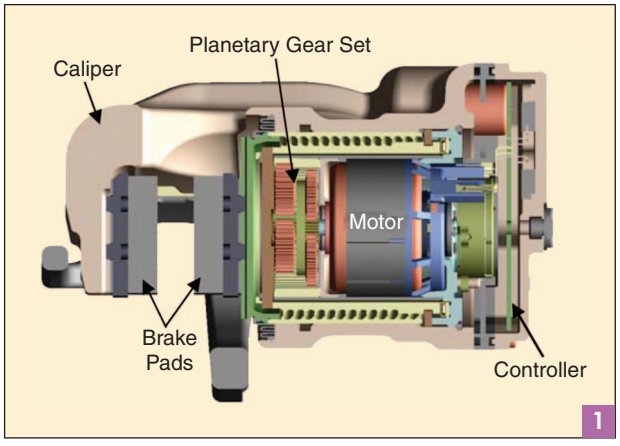

Sketch of the experimental EMB system.

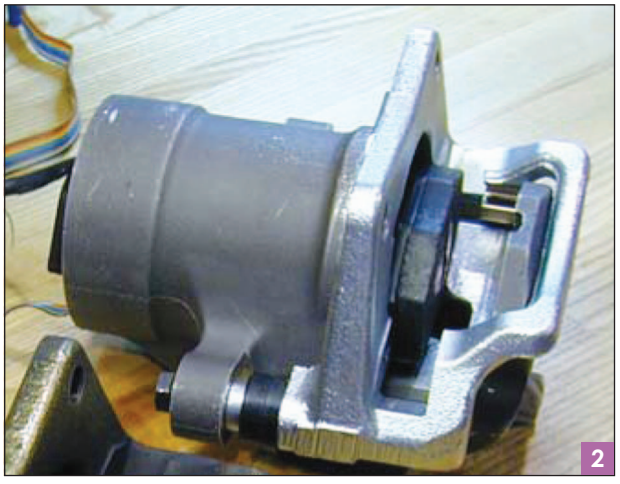

EMB, with the caliper bracket and brake pads removed. Motor fits inside housing.

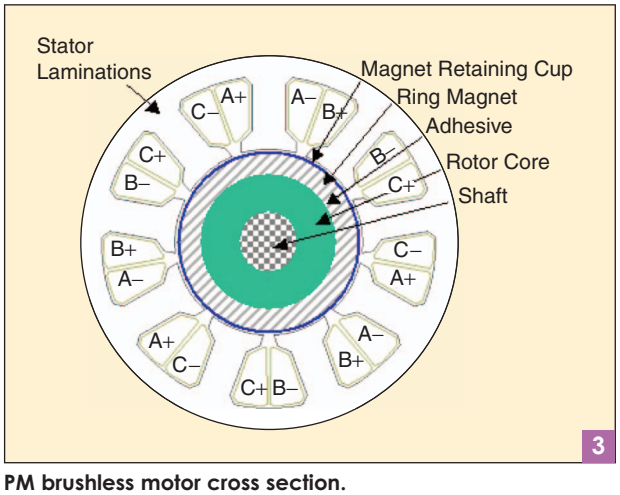

PM brushless motor cross section.

Design and Steady-State Performance

The SR and PM brushless motor designs are shown in cross-section in Figures 3 and 4. The PM brushless motor is based on the concentrated winding configuration, which is emerging as the design of choice when both high performance and low manufacturing costs are of concern [15], [16]. This configuration also has certain fault-tolerance advantages [3], and we used NdFeB magnets.

The SR motor is an 8/6 design. This 8/6 configuration provides good dynamic characteristics, in particular sufficient starting torque from any angular rotor position, an important feature for an EMB actuator. The resulting four phases normally require eight switches, although lower-cost configurations with six switches are possible [9]–[11].

Both motors have, by design, generally the same torque-speed characteristic (Figure 5; room temperature test data), with the notable and known exception of the high-speed capability of the SR motor (beyond 5,000 r/min in

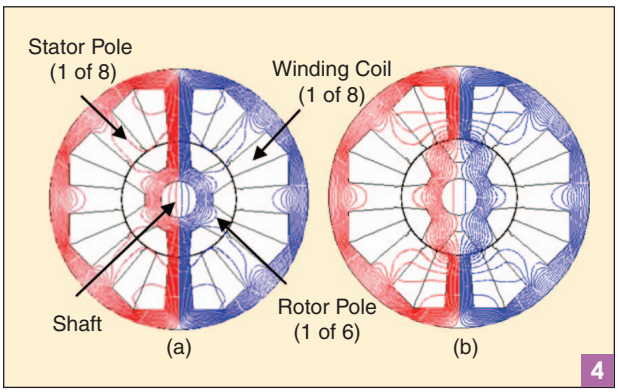

SR motor cross section with flux lines at (a) aligned and (b) unaligned positions.

Figure 5). To achieve this similar characteristic, the SR motor is 22% longer. The dc bus current of the SR motor at the 0.8-N·m point is higher by approximately 15% when compared against the PM brushless motor system. This difference, however, is largely offset at a higher temperature since the PM brushless motor torque constant drops with temperature (typically by at least 0.10%/°C for NdFeB magnets), while that of an SR motor is much less affected via the higher winding resistance.

The PM machine was driven by a classical trapezoidal approach, with Hall sensor feedback. Concerning the SR system, during this study, the motor was run with fixed firing angles: 27° span for first and third quadrants (acceleration) and 15° span for second and fourth quadrants (deceleration). The fixed firing angle scheme was motivated by the possibility of simplifying the controller, thus reducing its cost. Also, for reasons explained later, the motor is not expected to be used in the high-speed region where different angles might be necessary.

Another consideration for cost reduction was the use of relative rotor position to control the motor. This requires a special algorithm for startup, namely exciting one of the motor phases to align it, thus establishing a starting point reference [17].

Dynamic Performance

Test Setup and Load Description

The dynamic performances of the SR and PM brushless EMB systems were evaluated through a series of benchmark scenarios where the caliper is subjected to specific force commands. The selected scenarios test the system ability to respond fast (brake apply and release) and to change direction quickly from brake apply to brake release, and vice versa, as it occurs when road conditions change abruptly from dry to slippery, for instance. The evaluation also includes the back-drive capability of the motor-actuator system during a fault (e.g., loss of electric power). The data presented in this article are based on bench tests of an EMB prototype controlled with a dSpace system as shown in Figure 6.

In these tests, the same dc bus current limit was used for both motors. Also, for this specific bench setup, a force sensor was positioned between the brake pads. It measures the force that would be applied to the brake rotor and thus is the measure of the brake output, which is the object of the control.

A brake caliper, in essence, acts like a highly nonlinear spring acting against the motor (see Figure 7). As seen in this figure, at the onset of the motion profile, brake pads and force sensor are not mechanically engaged. This slight disengagement is necessary to operate the EMB with zero brake rotor drag for improved vehicle gas mileage. The amount of pad disengagement is adjusted dynamically as a function of the prevailing vehicle and brake system conditions (e.g., steady speed, disk wiping, and panic response). During the bench tests, however, it was set at a given, fixed distance from the sensor, equivalent to two motor revolutions.

The control of the brake force is therefore a dynamic positioning problem for a motor working against a highly nonlinear load. The force signal constitutes the outer loop control parameter, as shown in the block diagram in Figure 8. There are also two minor control loops: a current loop, to adjust the motor torque, and a motor position loop, for current turn-on and turn-off. Figure 8 shows a generic block diagram for both PM and SR motor-based EMB systems. For the PM-based system, the position feedback is based on 120° Hall sensors. For SR-based systems, the position feedback loop could use an encoder or be partially or fully sensorless [8], [17]. The inverter shown in Figure 8 is a three-phase full bridge inverter for

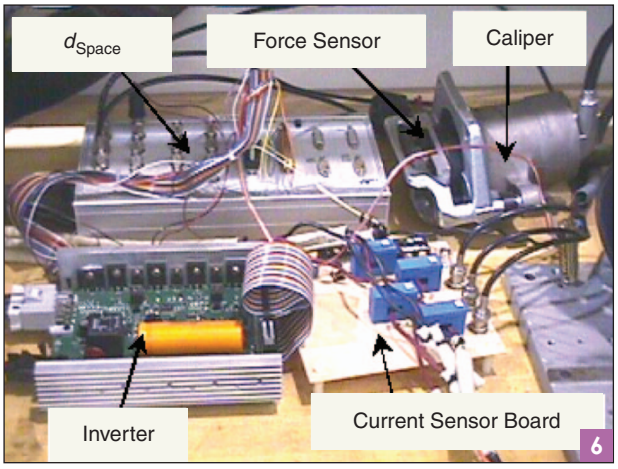

Photograph of test setup.

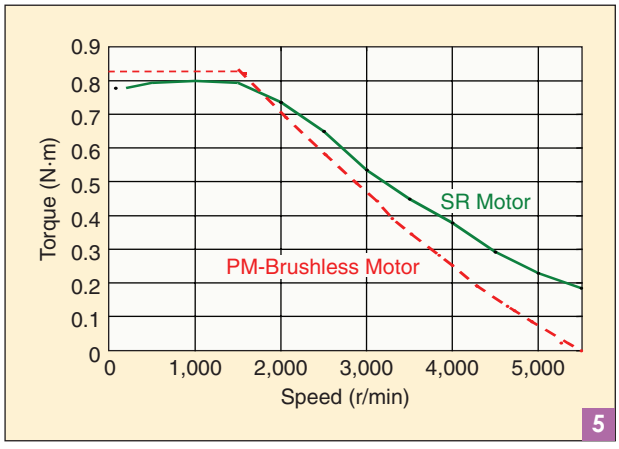

Comparison of torque-speed characteristics (test data).

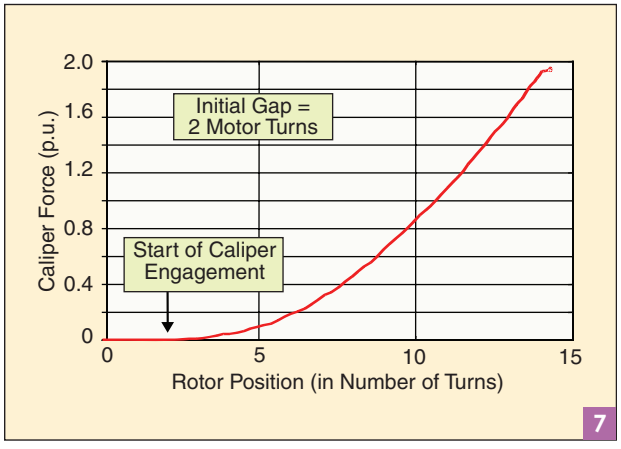

Caliper load characteristics.

TABLE 1. DYNAMIC PERFORMANCE OF PM BRUSHLESS AND SR EMBs.

	Apply (Figure 9)	Single Reversal (Figure 10)	Double Reversal (Figure 11)				Backdrive (Figure 12)
	Response Time (0–90%)	Overshoot Magnitude	Overshoot Magnitude	Overshoot Duration	Undershoot Magnitude	Undershoot Duration	Average Speed
PM EMB	181 ms	0.040 p.u.	0.022 p.u.	5 ms	0.040 p.u.	10 ms	16 p.u./s
SR EMB	187 ms	0.050 p.u.	0.020 p.u.	6 ms	0.045 p.u.	10 ms	22 p.u./s

PM drives or four-phase asymmetric half-bridge inverter for SR drives.

Brake Apply

Figure 9 shows a typical brake-apply pattern. As one can see on this plot, the SR motor is marginally slower at first, but both motors reach the command value in approximately the same time. The slower start of the SR motor may be attributed to a slightly smaller initial torque, since the motors were operated with the same dc bus current limit. However, both motors achieve approximately identical apply response times. Because of its lower initial speed, and because the SR-motor torque is higher than the torque of the PM brushless motor beyond base speed, the SR motor has more torque available later on, allowing it to catch up. Overall, both motors met the desired performance (specific numbers are presented in Table 1).

Proportional-integral differential (PID) parameters also have an effect when the system approaches the command value. Different sets of PID gains were used for the SR and PM actuators. The PID gains were tuned for each so that the specifications on the response time and overshoot or undershoot for the various scenarios are met. For example, higher PID gains will result in faster response time but also will result in higher overshoot and undershoot. So, the correct choice of the PID gains is a tradeoff between the two.

Brake Reversals

Figure 10 shows an example of a brake reversal, where the brake command is set to zero when the force reaches 0.4 per unit (p.u.). Figure 11 is a double reversal where the force command is set to zero at 1.5 p.u., and then reapplied when the force has reached 1.0 p.u.

What is measured in the reversal cases is the size (magnitude and duration) of the overshoot and undershoot. In this respect, the general conclusion was that the SR motor reversals are generally on par with those of the PM brushless motor (see Table 1), the difference being within event-to-event variations.

In Figures 10 and 11, the PM brushless motor reaches the reversal force levels sooner than the SR motor. Since these reversals occur at lower-force levels, the slightly slower SR motor response is therefore consistent with what was observed during the full apply scenario (Figure 9) where the SR motor catches up only at higher-force levels.

Back Drivability

The back-drivability test simulates a fault scenario under which the electric power to the actuator is shut off (open motor terminals), and brake release occurs solely via the

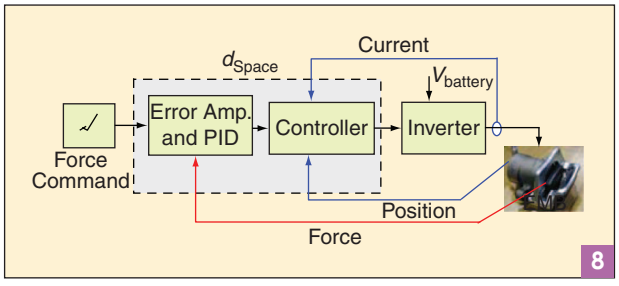

Generic block diagram of PM and SR test setups.

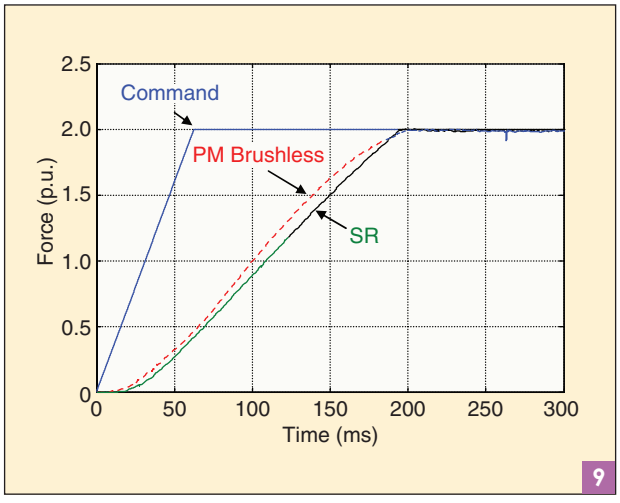

Comparison of brake apply performance (test data).

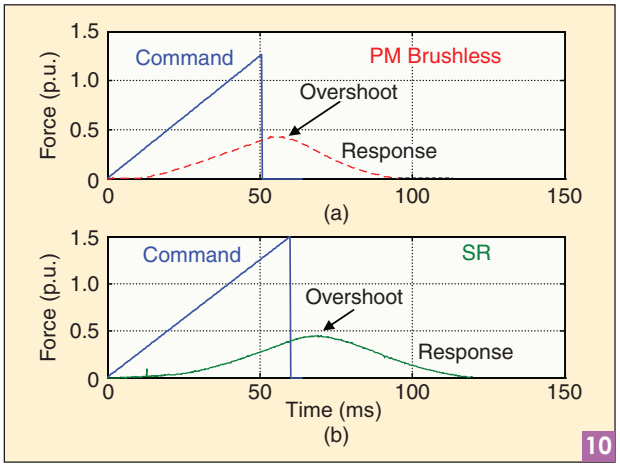

Single-reversal performance of brake (test data). (a) PM brushless EMB. (b) SR EMB.

spring energy stored in the caliper. Fast back-drivability is a desirable brake feature since it makes it possible for the system to fall silent, which requires auto-release of a faulty brake at the highest possible rate.

The SR motor has, with respect to back drivability, an advantage over the PM brushless motor, as shown in Figure 12. The SR system backdrives from full brake force at a rate of 22.0 p.u./s versus 16.0 p.u./s for the PM brushless motor. The latter is slower because of the always present flux in the motor and the magnetic losses associated with it, while the SR motor defluxes immediately upon turn-off.

Energy Requirement

The average electrical energy needed for an EMB motor to operate the brake under typical driving conditions is considered to be insignificant when compared against other electrical loads, because brake operation is very intermittent. Therefore, energy is of importance only as it relates to peak power consumption, heat generation, and motor or controller design. Although the motor energy is by many magnitudes smaller than the energy that is generated by the brake itself, it is still relevant in terms of localized short-term losses and self-heating effects in the motor.

The energy used by the PM brushless and SR motors was thus measured for the record. This was done by moving the motor slowly over a linearly increasing force ramp, from standstill to some force level (1.5 p.u.) in 5 s, then driving it back slowly and symmetrically to its initial position. These slow ramps are chosen to create a quasi-static load scenario and prevent particular dynamic patterns that occur during fast operation, which could dominate the energy need and skew the results.

The cumulative energy required by the PM brushless and SR EMBs during the above test cycle is plotted in Figure 13. The SR caliper used 575 J versus 410 J for the PM system. PM brushless motors are generally more efficient than SR motors, thanks to the use of magnets for excitation. A 40% difference, however, is larger than expected. Reasons for this greater than expected difference can be found in the fact that the SR motor was designed for dynamic operation, rather than efficiency, and used fixed controller firing angles during the experiments.

SR Motor Implementation with Speed Limit

Need for Motor Speed Limit

An important finding of this work was that, in order to achieve an appropriate EMB reversal behavior, the SR system must impose a speed limit on the motor [18]. This section will demonstrate this need, and how to derive the necessary speed limits for forward and reverse directions.

The various EMB performance comparisons made in the previous sections, including the test data, were done with speed limits of 5,000 r/min (forward direction) and 3,500 r/min (reverse direction) imposed on the SR motor, through software.

For the purpose of comparison, two brake reversal patterns, with and without speed limits, were modeled with a MATLAB/Simulink model (described in [2]). Figure 14 compares the system behavior (a) with and (b) without a speed limit, for a single reversal. The overshoot magnitudes are 0.24 and 0.70 p.u., respectively, almost three times larger without speed limit.

Figure 15 is a more dramatic demonstration of the need for a speed limit. In a double reversal test without a speed limit, the brake is fully released (compare Figure 11 where a speed limit was used). The second reversal is more difficult, because the caliper exerts a spring force that tends to release the brakes, working against the motor when the brake command is reapplied. Of course, the brake could be reengaged, but such delay is not acceptable.

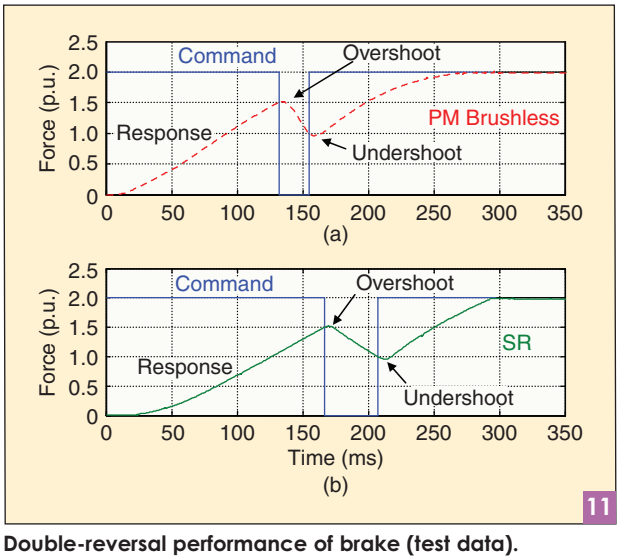

Double-reversal performance of brake (test data). (a) PM brushless EMB. (b) SR EMB.

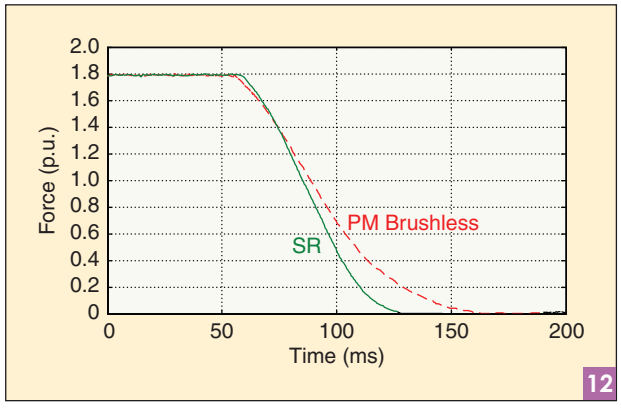

Back-drivability test.

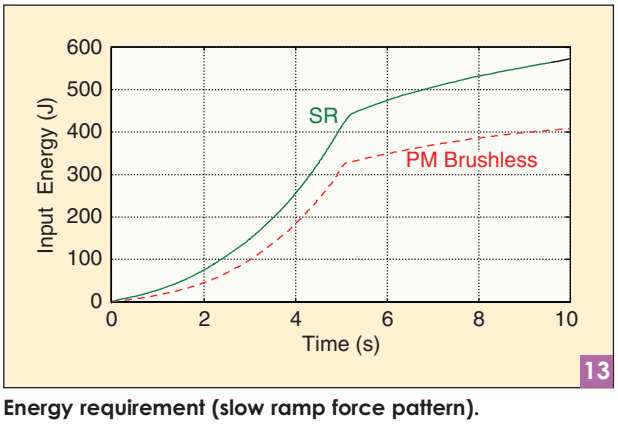

Energy requirement (slow ramp force pattern).

The need for a speed limit for SR motors can be understood as follows. SR motors have a torque-speed characteristic that includes some torque capability at speeds exceeding the no-load speed of an equivalent PM brushless motor, as already depicted in Figure 5. This is an advantage when the motor is used in a steady-state manner. However, if an unexpected motion-reversal command occurs while the motor is at high speed, one faces a situation which combines a high system kinetic energy with little torque available to overcome the momentum.

By contrast, the no-load speed of the PM brushless motor constitutes an absolute limit. At low loads, the motor speed and thus the system kinetic energy are limited, making it easier to reverse motion. Furthermore, with a PM brushless motor, as the reversal process starts and the motor slows down, the torque increases more rapidly compared to that of an SR motor, thus amplifying the deceleration process.

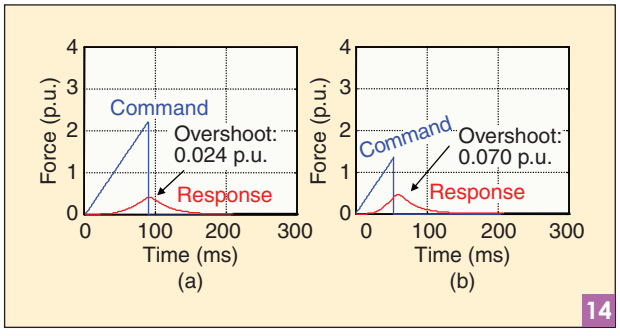

Brake reversal (a) with and (b) without speed limits for the SR motor (model).

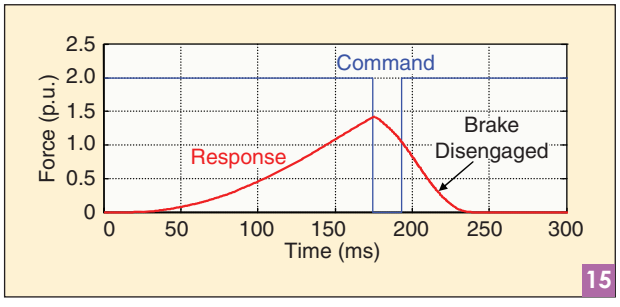

Double-brake reversal without speed limit for the SR motor (model).

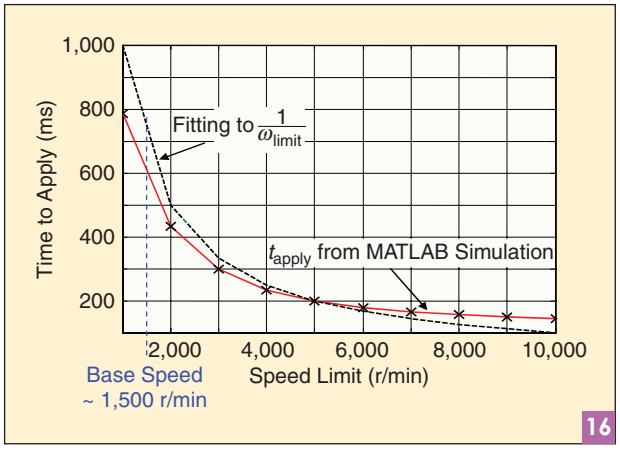

Apply time versus motor speed limit.

Impact of Motor Speed Limits on Performance

A practical question, then, consists of selecting the top speed that should be designed into or chosen for the motor. A low-speed limit helps with motion reversals but hampers normal brake applies and releases, and vice-versa. Also, because of the caliper spring action, forward and reverse directions are not symmetrical, and therefore one may choose different speed limits for both. A theoretical study was thus conducted on the basis of two models: a MATLAB/Simulink model (with nonlinear effects included, such as caliper force and motor switching models [2]) and a simplified kinematics model (derived in "Derivations for Apply Time and Reversal Overshoots and Undershoots").

Results of the MATLAB/Simulink model are shown in Figures 16–18, with apply time (Figure 16) and overshoot and undershoot magnitude and duration during motion reversals (overshoot shown in Figure 17; undershoot in Figure 18), as a function of the speed limit imposed on the motor. In an effort to generalize the results presented here as much as possible, the motor base speed is shown as a reference point. These results can be understood with the help of the simplified model derived in detail in "Derivations for Apply Time and Reversal Overshoots and Undershoots". According to that model, the time to apply is (A10):

$$t_{\text{apply}} \approx \frac{\theta_{\text{f}}}{\omega_{\max}}, \tag{1}$$

where θ_{f} is the motor position when the maximum braking force is reached, and $\omega_{\max}$ the proposed speed limit of the motor. The (1/speed limit) relationship in (1) is indeed observed with the MATLAB model (Figure 16). Since the motor speed is clamped at $\omega_{\max}$, (1) is valid as the motor acceleration at that point is close to zero. The duration t_{os} and magnitude θ_{os} of an overshoot during reversals can be

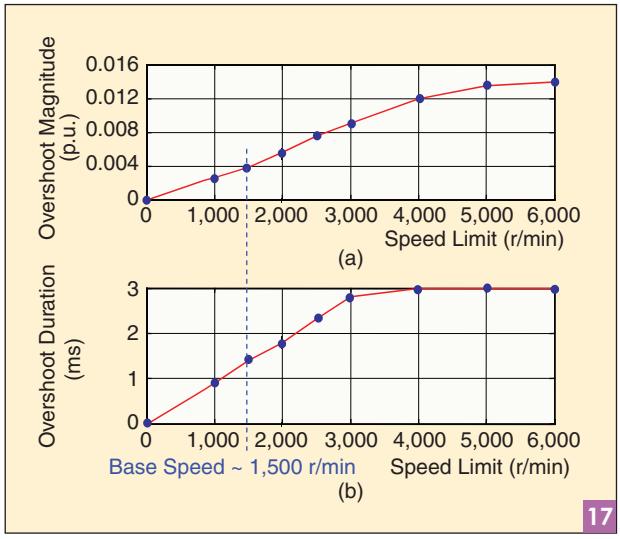

Overshoot (a) magnitude and (b) duration during motion reversals versus motor speed limit.

similarly calculated to be [(A13) and (A14)].

$$t_{os} = \frac{2J}{(T_M + T_{cal})}\omega_{max} \quad \text{and} \qquad (2)$$

$$\theta_{os} = \frac{J}{(T_M + T_{cal})}\omega_{max}^2, \text{respectively,} \qquad (3)$$

where J is the system inertia, and T_M and T_{cal} the motor torque and caliper reaction torque (as seen from the motor), respectively. The undershoot duration and magnitude after a second reversal are [(A16) and (A17)]:

$$t_{us} = \frac{2J}{(T_M - T_{cal})}\omega_{max} \quad \text{and} \qquad (4)$$

$$\theta_{us} = \frac{J}{(T_M - T_{cal})}\omega_{max}^2. \qquad (5)$$

The overshoot and undershoot durations are linear with speed limit,

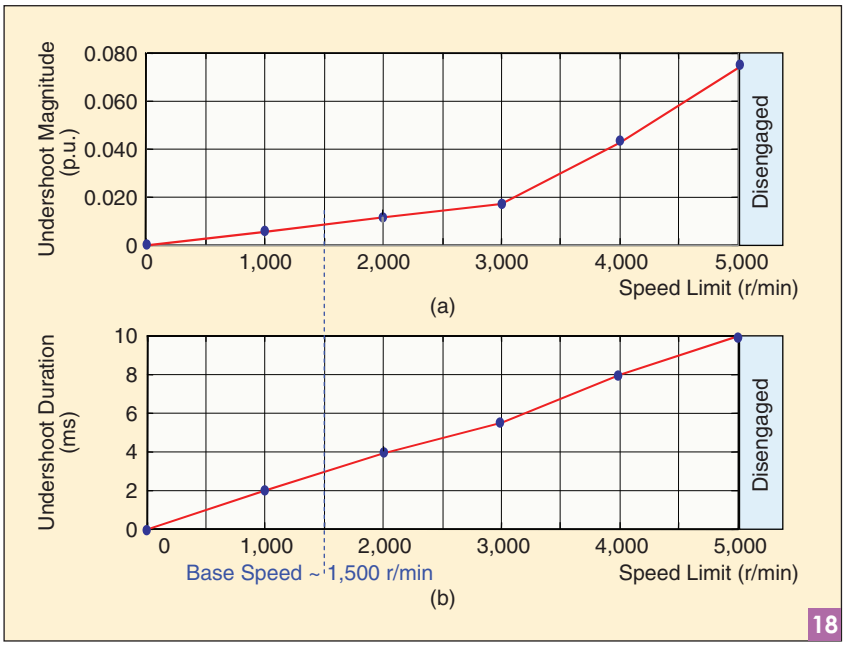

(a) Magnitude and (b) duration of reapply reversal undershoot versus motor speed limit.

DERIVATIONS FOR APPLY TIME AND REVERSAL OVERSHOOTS AND UNDERSHOOTS

The purpose of this section is to derive simple equations linking the time to apply, and the reversal overshoot and undershoot magnitudes, to the maximum motor speed.

Time to Apply

The time to apply is the time to reach the system maximum force F_f. This maximum force level corresponds to some motor angular position, dubbed θ_f. The time to apply, therefore, is the time it takes for the motor to reach θ_f. At the start of motion, the system kinematics can be approximated by the following equation:

$$J\dot{\omega} = T_M - T_L, \qquad (A1)$$

where J is the system inertia (motor, gears, etc.) reflected back to the motor, T_M is the motor torque and T_L is the load torque, mostly the caliper reaction force. The caliper reaction force, however, is not present until the caliper pads actually engage the rotor, and is small at first. For a good part of an apply sequence, therefore, there is no load torque and motion can be approximated by

$$J\dot{\omega} = T_M. \qquad (A2)$$

The motion, then, can be divided into two separate times, first, acceleration up to maximum speed ω_{max}, then motion at constant speed. Assuming for simplicity that the motor torque is constant and determined by the inverter current limit, the first acceleration, until $\omega = \omega_{max}$, is governed by

$$\omega = \frac{T_M}{J}t \quad \text{and} \qquad (A3)$$

$$\theta = \frac{T_M}{2J}t^2, \qquad (A4)$$

and the time t_1 and position θ_1 corresponding to when ω has reached ω_{max} are

$$t_1 = \frac{J}{T_M}\omega_{max} \quad \text{and} \qquad (A5)$$

$$\theta_1 = \frac{J}{2T_M}\omega_{max}^2. \qquad (A6)$$

After time t_1, the motor runs at constant speed:

$$\theta - \theta_1 = \omega_{max}(t - t_1). \qquad (A7)$$

The total travel time t_f to reach the final position θ_f is thus given by

$$\theta_f = \theta_1 + \omega_{max}(t_f - t_1). \qquad (A8)$$

Combining (A5) and (A6) into (A8) yields, after some manipulation,

$$t_f = \frac{\theta_f}{\omega_{max}} + \frac{J}{2T_M}\omega_{max}. \qquad (A9)$$

and their magnitudes are quadratic with speed limit. This is borne out by the MATLAB model, except perhaps for the overshoot magnitude, which is somewhat less than quadratic, probably because of simplifications. Comparing overshoots and undershoots, the latter are larger because of the caliper torque that acts with the motor during a first reversal and against the motor when the brake is reapplied. This appears in the above equations as a different denominator for (2) and (3), on one hand, and (4) and (5), on the other.

The overshoot duration and magnitude reach a plateau at some level, when the motor speed is limited anyway by the system load, such as the caliper reaction force. Concerning undershoot, it can grow rapidly because of the help from the caliper spring force, to the point that the brake can become fully disengaged. Such a disengagement is shown in Figure 15.

Motor Speed Limit Selection

The motor speed limits can now be chosen as follows. Concerning forward motion, and referring first to the apply time, based on Figure 16, it is logical to choose a speed limit in the 4,000–6,000 r/min range, because below such levels significant sacrifices are made in apply time. In that

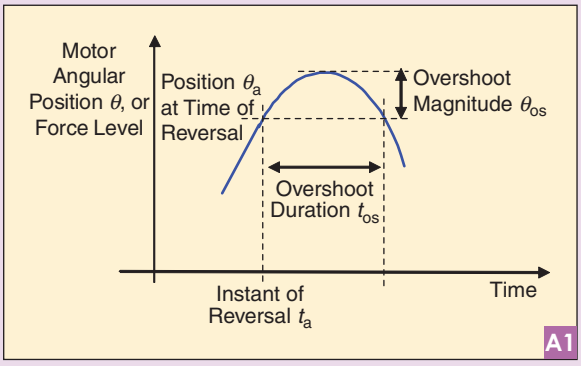

Overshoot pattern.

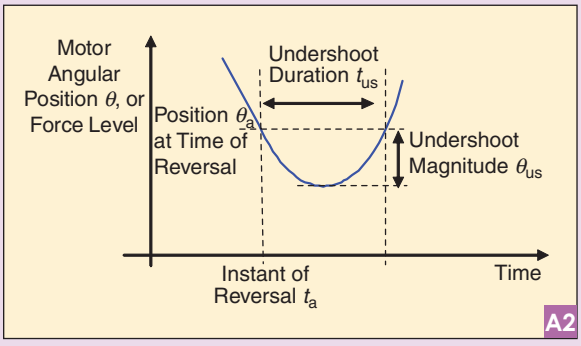

Undershoot pattern.

By design, these systems have a high torque-per-inertia ratio; therefore, the first term is dominant (A11). This establishes a (1/speed limit) pattern for the time to apply. It also shows that, provided the torque per inertia is sufficiently high, only higher motor speeds can shorten the time to apply.

$$t_{apply} = t_f \approx \frac{\theta_f}{\omega_{max}}. \qquad \text{(A10)}$$

Overshoot Pattern Reversal

When the brake reverses motion from forward to reverse, an overshoot occurs with a generally parabolic shape, as shown in Figure A1. During the overshoot, the motor is decelerated by a negative motor torque, $-T_M$, which adds to the caliper force, T_{cal}, leading to

$$J\dot{\omega} = -T_M - T_{cal}. \qquad \text{(A11)}$$

The reversal occurs as the motor runs at its maximum speed ω_{max}. Although the caliper torque is nonlinear with position, for simplicity it will be assumed constant, as well as the motor torque, during the reversal. Then, the motor position is

$$\theta - \theta_a = -\frac{(T_M + T_{cal})}{2J}(t - t_a)^2 + \omega_{max}(t - t_a). \qquad \text{(A12)}$$

The duration t_{os} of the overshoot, defined as the time $t_{os} = (t - t_a)$ for the angle θ to be again equal to θ_a, is

$$t_{os} = \frac{2J}{(T_M + T_{cal})}\omega_{max}. \qquad \text{(A13)}$$

The overshoot magnitude θ_{os} corresponds to when the angle function starts to decrease, and therefore to when the derivative of position (A12) is zero. After some manipulation,

$$\theta_{os} = \frac{J}{(T_M + T_{cal})}\omega_{max}^2. \qquad \text{(A14)}$$

Undershoot Pattern for Second Reversal (Reapply)

The analysis when a brake is required to reverse motion from a reverse direction (release) to forward (apply) is similar. The resulting undershoot also has a generally parabolic shape, as shown in Figure A2.

The main difference is that in this case, the motor torque tries to accelerate the motor in the forward direction while the caliper torque still acts in the opposite direction; therefore,

$$J\dot{\omega} = T_M - T_{cal}. \qquad \text{(A15)}$$

Assuming again constant motor and caliper torques during the reversal, the undershoot duration t_{us} and magnitude θ_{us} are

$$t_{us} = \frac{2J}{(T_M - T_{cal})}\omega_{max} \quad \text{and} \qquad \text{(A16)}$$

$$\theta_{us} = \frac{J}{(T_E - T_{cal})}\omega_{max}^2. \qquad \text{(A17)}$$

range, the overshoot is little affected. If the resulting values of apply time or overshoot are not satisfactory, a system redesign is in order (either motor, brake system, or both). In this case, the final choice of 5,000 r/min provided acceptable EMB performance results.

Concerning reverse motion, a speed limit of 5,000 r/min would be unstable, as seen in Figure 18. A lower value, in the knee of the undershoot magnitude (at 3,500 r/min) was chosen. This choice has an effect on the release time for the brake. The release time was also analyzed, in the same way as apply time. This analysis is omitted here for conciseness.

The two speed limits, one for forward and one for reverse direction, are generic conditions that are used in the controller. When the speed limit is reached, one switch is turned off to allow the motor to coast down. The forward speed limit is higher since the motor has to work against the spring force and the reverse speed limit is lower since the spring force aids the force produced by the motor actuation. Clearly, the speed-limit values will change depending on the application, but the method proposed here was presented in hopefully the most general terms to help in future such designs. Also, the base speed (1,500 r/min) is noted as a possible point of reference.

The approach was qualitatively confirmed by adjusting the speed limits during testing, while at the same time the PID parameters were being tuned. As was mentioned earlier, the final choices, 5,000 and 3,500 r/min, are generally consistent with the analysis. Most notably, however, the SR motor could not have met the reversal needs without such an approach.

Conclusions

This study challenged both a PM brushless and an SR motor in highly dynamic situations, in all four quadrants of their torque-speed operating regions, for an EMB application. A 20% longer SR motor provided overall similar dynamic performance, but only if the SR motor is fitted with a speed limit. A method to choose such a speed limit was developed, and the software algorithm implementation was found to be simple and successful.

Acknowledgments

The authors are indebted to Dr. Syed Hossain, Dr. Ahmed Khalil, and Dr. Samuel Underwood (former Ph.D. students of the University of Akron) and to their Delphi colleagues, Mr. Lonnie Frost, Mr. Erik Nedelcu, and Mr. Stan Rawski. This research was conducted while Omekanda, Lequesne, Klode, and Gopalakrishnan were with Delphi Corporation, Troy, Michigan, on contract with Husain and the University of Akron.

References

[1] M. Kees, K. J. Burnham, F. P. Lockett, J. H. Tabor, and R. A. Williams, "Hydraulic actuated brake and electromechanically actuated brake systems," in *Proc. Int. Conf. Advanced Driver Assistance Systems*, 2001, pp. 43–47.

[2] S. Underwood, A. Khalil, I. Husain, H. Klode, B. Lequesne, S. Gopalakrishnan, and A. M. Omekanda, "Switched reluctance motor based electromechanical brake-by-wire system," *Int. J. Veh. Auton. Syst.*, vol. 2, no. 3/4, pp. 278–296, 2004.

[3] A. G. Jack, B. C. Mecrow, and J. Haylock, "A comparative study of PM and SR motors for high performance fault tolerant applications," *IEEE Trans. Ind. Applicat.*, vol. 32, no. 4, pp. 889–895, 1996.

[4] K. Atallah, F. Caparrelli, C. M. Bingham, P. H. Mellor, C. Cossar, L. Kelly, P. Kjaer, J. Gribble, T. J. E. Miller, R. Capewell, and C. Whitley, "Comparison of electrical drive technologies for aircraft flight control actuation," presented at the 9th Int. Conf. Electrical Machines and Drives, 1999, Paper no. 468.

[5] W. Cai, "Starting engines and powering electric loads with one machine," *IEEE Ind. Applicat. Mag.*, vol. 12, no. 6, pp. 29–38, Nov./Dec. 2006.

[6] E. Richter and C. Ferreira, "Performance evaluation of a 250-kW switched reluctance starter generator," in *Proc. 30th IEEE Industry Applications Society Annu. Meet.*, 1995, vol. 1. pp. 434–440.

[7] S. A. Hossain, I. Husain, H. Klode, B. Lequesne, A. M. Omekanda, and S. Gopalakrishnan, "Four-quadrant and zero-speed sensorless control of a switched reluctance motor," *IEEE Trans. Ind. Applicat.*, vol. 39, no. 5, pp. 1343–1349, Sept./Oct. 2003.

[8] A. Khalil, S. Underwood, I. Husain, H. Klode, B. Lequesne, S. Gopalakrishnan, and A. M. Omekanda, "Four quadrant pulse injection and sliding-mode-observer-based sensorless operation of a switched reluctance machine over entire speed range including zero speed," *IEEE Trans. Ind. Applicat.*, vol. 43, no. 3, pp. 714–723, May/June 2007.

[9] S. Vukosavic and V. R. Stefanovic, "SRM inverter topologies: A comparative evaluation," *IEEE Trans. Ind. Applicat.*, vol. 27, no. 6, pp. 1034–1047, Nov./Dec. 1991.

[10] M. Barnes and C. Pollock, "Power electronic converters for SR drives," *IEEE Trans. Power Electron.*, vol. 13, no. 6, p. 1100, Nov. 1998.

[11] A. Khalil, I. Husain, S. A. Hossain, S. Gopalakrishnan, A. M. Omekanda, B. Lequesne, and H. Klode, "A hybrid sensorless SRM drive with eight- and six-switch converter topologies," *IEEE Trans. Ind. Applicat.*, vol. 41, no. 6, pp. 1647–1655, Nov./Dec. 2005.

[12] A. M. Omekanda, "Robust torque and torque-per-inertia optimization of a switched reluctance motor using the Taguchi methods," *IEEE Trans. Ind. Applicat.*, vol. 42, no. 2, pp. 473–478, Mar./Apr. 2006.

[13] H. Klode, A. M. Omekanda, B. Lequesne, S. Gopalakrishnan, A. Khalil, S. Underwood, and I. Husain, "The potential of switched reluctance motor technology for electro-mechanical brake applications," presented at the SAE World Congress, Apr. 3–6, 2006, Paper 2006-01-0296.

[14] D. B. Drennen, E. R. Siler, G. C. Fulks, and D. E. Poole, "Caliper with internal motor," U.S. Patent 6 626 270 B2, Sept. 30, 2003.

[15] F. Magnussen and H. Lendenmann, "Parasitic effects in PM machines with concentrated windings," *IEEE Trans. Ind. Applicat.*, vol. 43, no. 5, pp. 1223–1232, Sept./Oct. 2007.

[16] H. Akita, Y. Nakahara, N. Miyake, and T. Oikawa, "A new core," *IEEE Ind. Applicat. Mag.*, vol. 11, no. 6, pp. 38–43, Nov.–Dec. 2005.

[17] B. Lequesne, A. Omekanda, S. A. Hossain, H. Klode, and J.-J. Chen, "Switched reluctance motor control," U.S. Patent application SSN 20030042864, Mar. 6, 2003.

[18] S. A. Hossain, I. Husain, B. Lequesne, A. Omekanda, and H. Klode, "Controlling an electric motor," U.S. Patent 7 042 189, May 9, 2006.

Avoki M. Omekanda (avoki.m.omekanda@delphi.com) is with Delphi Advanced Powertrain Systems in Auburn Hills, Michigan. Bruno Lequesne is with the University of Alabama in Tuscaloosa, Alabama. Harald Klode is with Goodrich Aircraft Wheels and Brakes in Troy, Ohio. Suresh Gopalakrishnan is with General Motors R&D Center in Warren, Michigan. Iqbal Husain is with the University of Akron in Akron, Ohio. Omekanda and Lequesne are Fellows of the IEEE. Gopalakrishnan and Husain are Senior Members of the IEEE. This article first appeared as "Switched Reluctance and Permanent Magnet Brushless Motors in Highly Dynamic Situations: A Comparison in the Context of Electric Brakes" at the 2006 IEEE Industry Applications Society Electrical Machines Conference.